

Application of matrix analysis for structural calculation of support base for hydraulic gate drive piston

Aplicação de análise matricial para cálculo estrutural de base de suporte para pistão de acionamento de comporta hidráulica

Henrique Batista Redin¹, Raphael Basilio Pires Nonato^{2*}

RESUMO

A disponibilidade de energia elétrica é crucial para o desenvolvimento de um país, sendo a geração por usina hidrelétrica a mais importante no Brasil. Portanto, este artigo visa aumentar a velocidade de cálculo preliminar para a etapa de orçamentação de uma base para suporte de pistão hidráulico de comporta hidráulica por meio da aplicação da análise matricial (AM). Este trabalho classifica-se como pesquisa aplicada, pois trata-se de uma verificação estrutural limitada a uma aplicação específica. No que se refere à forma de abordagem, a pesquisa classifica-se como quantitativa, por aplicar um método de verificação e obter valores numéricos de resposta e, também, comparar com valores numéricos admissíveis por norma. Em relação aos objetivos da pesquisa, considera-se como descritiva, pois elabora uma rotina para verificação estrutural de uma base de suporte. Utilizando o Python[®], o Ansys[®] e a AM, o tempo de análise representa agora somente 11,6% do tempo obtido via método dos elementos finitos com uma perda de acuracidade de 5,6% em tensão.

Palavras-chave: Hidrelétrica. Comporta Vagão. Análise Matricial. Método dos elementos finitos.

ABSTRACT

The availability of electrical energy is crucial for developing a country, making the generation by hydroelectric plants the most important in Brazil. Therefore, this paper aims to reduce the time of preliminary calculation for the budgeting stage of a base for supporting a hydraulic piston of a hydraulic gate through the application of matrix analysis (MA). This work is classified as applied research, focusing on structural verification limited to a specific application. In terms of approach, the research is quantitative, employing a verification method to obtain numerical response values and comparing them with norm-admissible numerical values. Concerning the research objectives, it is considered descriptive, as it develops a routine for the structural verification of a support base. Using Python[®], Ansys[®], and MA, the analysis time now represents only 11.6% of the time obtained via the finite element method with a loss of accuracy of 5.6% in stress.

Keywords: Hydroelectric plant. Hydraulic gate. Matrix Analysis. Structural calculation. Finite element method.

¹ Bachelor. Mechanical Engineering. Federal Institute of Santa Catarina (IFSC), Xanxerê. <https://orcid.org/0009-0004-1618-3363>.

² D.Sc. Technological and Environmental Processes. Federal Institute of Santa Catarina (IFSC), Chapecó. <https://orcid.org/0000-0002-4740-9888>.

E-mail:

raphaelbasilio@gmail.com

1. INTRODUCTION

Electrical energy from hydraulic generation is responsible for 58% of the total installed capacity in operation in Brazil. This shows that the hydroelectric branch is of great importance for the energy matrix of the country. Furthermore, 40% of the potential for generating electrical energy through hydraulic generation has not yet been used (ANEEL, 2023). This shows that, even though Brazil has many hydroelectric plants in operation, there are still opportunities in this business field.

One of the groups of equipment responsible for the operation in a hydroelectric plant is the so-called hydraulic gate (Figure 1a), whose parts that make up a gate are the deck, the fixed parts, and the maneuvering mechanism (Figure 1b) (ERBISTI, 2008).

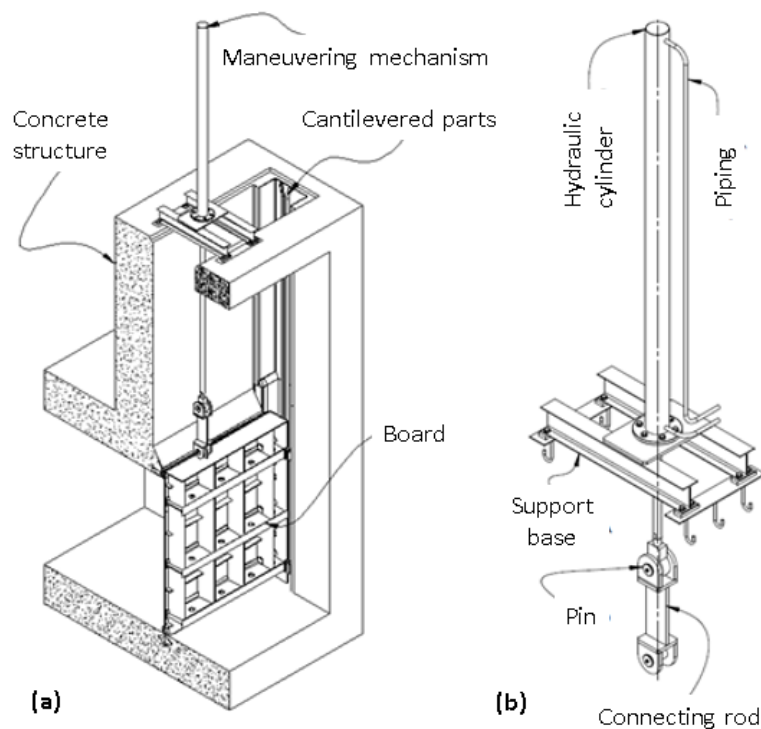


Figure 1. (a) Main components of a hydraulic gate; (b) maneuvering mechanism.

In addition to the support base, this assembly encompasses the hydraulic cylinder, piping, connecting rod, and pin. The hydraulic cylinder is actuated by an oil pump, which lowers (closes) or raises (opens) the board via a connecting rod. The support base sustains the maneuvering mechanism, transferring the pressure loading to a grounded structure.

The hydraulic system is one of the solutions to operate the equipment responsible for the maneuver. This system consists of a hydraulic piston, pipes and connections, a hydraulic unit responsible for control, and a support base (ERBISTI, 2008).

The support base that sustains the load applied by the piston is of great importance for the operation of the gate, as well as for the safety of the plant. Therefore, it must be structurally verified and demand as little time as possible.

Matrix analysis (MA) is applied in many branches of structural calculation. A reduced-order extrapolated technique was applied to find the coefficient vectors of solutions in the finite element method (FEM) (LUO; JIANG, 2020). Two similar works also refer to a reduced-order approach to finding the unknown vectors in the FEM via MA (TENG; LUO, 2021) (ZENG; LUO, 2022). A proper orthogonal decomposition was employed to lower the dimensionality of the unknowns of FEM for the fractional Tricomi-type equation, in which MA is applied (LI; LUO, 2023).

The time spent to obtain accurate dimensional verification for the budgeting phase is crucial. The more accurate and faster the method, the greater the competitiveness in a mature market. Therefore, there must be faster and more accurate manners to obtain structural verification results of the support base for hydraulic cylinders.

The calculation of the support base can be made using the finite element method (FEM), in which a model should be prepared to be run. However, the creation and preparation of this model frequently demands an excessive amount of time. To reduce the time spent in the budgeting process, MA is proposed herein as an alternative to keep the calculation accuracy within a certain level and concomitantly reduce the time elapsed in the calculation process, which is part of the budgeting one.

Therefore, this paper aims to reduce the time spent on preliminary calculation for the budgeting stage of a support base (for supporting a hydraulic piston of a hydraulic gate) by applying MA in the context of structural verification. This is accomplished under the hypothesis of being possible to code a program in which it is faster to fill it in than to perform a finite element analysis (FEA).

2. MATERIALS AND METHODS

The proposed methodology starts with the definition of the design of the support base (including geometry and material) and its boundary conditions. Then, the global stiffness matrix is assembled from each elementary stiffness matrix, as well as the load matrix and the displacement matrix. Thenceforth, the nodal displacements and the internal loads are obtained via MA. After this is accomplished, the stress is calculated, and a FEA is performed. At this stage, the results from MA and FEA are then compared.

The design adopted for the support base can be seen in Figure 2. The support base is composed of two parallel beams and a plate to accommodate the hydraulic cylinder.

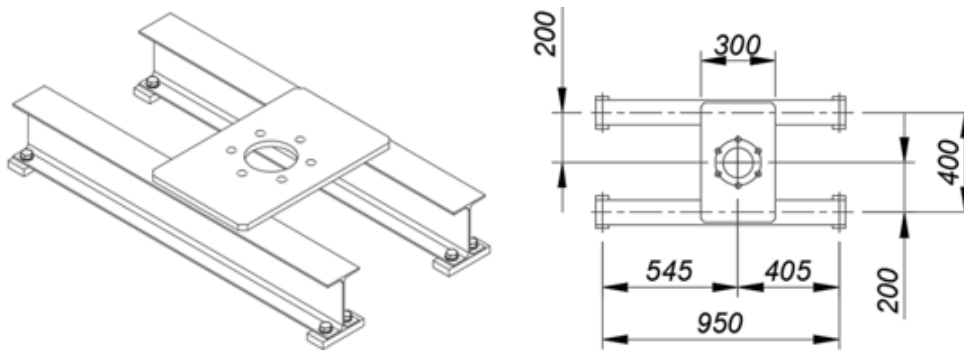


Figure 2. Support base design, in which dimensions are in *mm*.

In what refers to its boundary conditions, as shown in Figure 2, the support base is assembled on metal anchors joined with concrete. This causes the ends of the beams to be modeled as clamped in a small area at the bottom of the beams. The piston is screwed to the plate that is welded above the beams and applies a vertical load normal to the plane of the plate's largest dimensions.

Nodes and elements are identified in Figure 3. The nodes are represented by the letter “*N*”, the elements by “*E*”, and the force by F_1 . The local coordinates for the structural elements are also represented.

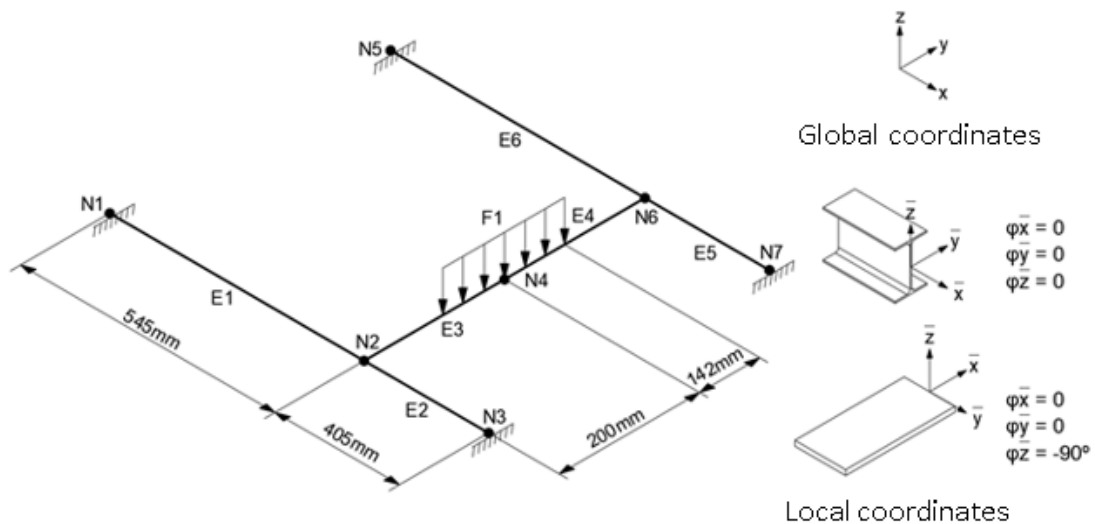


Figure 3. Nodes, elements, and coordinate systems for the support base.

Elements 1, 2, 5, and 6 are equivalent to the structure's beams, while elements 3 and 4 refer to the plate. For the boundary conditions presented, nodes 1, 3, 5, and 7 are delimited without displacement, reflecting the clamping condition.

The value of 25 kN was estimated as the load applied. The material ASTM A36 was selected for the plate and ASTM A572 Gr. 50 for the beams. Table 1 presents the values of the properties of the chosen materials, in which S_y is the material yield strength. The selection of materials was based on typical commercial materials for this type of application.

Table 1. Materials properties.

Material	E (GPa)	G (GPa)	S_y (MPa)
ASTM A36	207	80	250
ASTM A572	207	80	345

Source: CALLISTER, W. D; RETHWISCH, 2012.

The thickness of the selected plate was 3/4 in (19.05 mm) and the beam selected was the W200 x 22.5 one. Table 2 refers to the inertia moments of the plate and beam.

Table 2. Inertia moments.

Section	I_y (m ⁴)	I_z (m ⁴)	J (m ⁴)
#19.05	1.95×10^{-5}	7.93×10^{-10}	5.10×10^{-8}
W200 x 22.5	1.42×10^{-6}	2.03×10^{-5}	2.17×10^{-5}

Source: GERDAU, 2023.

I_y is the inertia moment related to y axis, and I_z is the inertia moment related to z axis. The entire calculation was solved using the Python[®] programming language with the help of the SymPy[®] library in the Jupyter Notebook interface. This was justified due to the size of the matrices and the number of linear equations generated by these matrices. This includes the application of the solve function from the library to solve the linear system and obtain the displacements.

After obtaining the elementary stiffness of all elements about the global coordinates, the assemblage process takes place. To accomplish this, it is necessary to assemble the table that relates each element with the nodes equivalent to nodes i and j .

The elementary stiffness matrix can be divided into four submatrices, k_{ii}^n , k_{ij}^n , k_{ji}^n , and k_{jj}^n , where the indices i and j represent the nodes that constitute element n . These four submatrices with their respective indices assign the contributions of each element in the global stiffness matrix. Furthermore, these matrices have dimensions of 3x3. Subsequently, to assemble the global stiffness matrix, a square matrix was created equivalent to the

number of nodes, i.e. 7×7 . Thenceforth, based on the indices obtained in Table 3, it is possible to determine how each element contributes to the global matrix.

Table 3. Identification of the assemblage of the involved elements.

Element	Node i	Node j	k_{ii}^n	k_{ij}^n	k_{ji}^n	k_{jj}^n
1	1	2	k_{11}	k_{12}	k_{21}	k_{22}
2	2	3	k_{22}	k_{23}	k_{32}	k_{33}
3	2	4	k_{22}	k_{24}	k_{42}	k_{44}
4	4	6	k_{44}	k_{46}	k_{64}	k_{66}
5	6	7	k_{66}	k_{67}	k_{76}	k_{77}
6	5	6	k_{55}	k_{56}	k_{65}	k_{66}

Therefore, the values obtained in the elementary stiffness matrices must be replaced in the global stiffness matrix. Each value represented in the global stiffness matrix has the dimension of 3×3 and its location as shown in Equation 1. A 21×21 matrix was then obtained for the global stiffness matrix.

$$K = \begin{pmatrix} k_{ii}^1 & k_{ij}^1 & 0 & 0 & 0 & 0 & 0 \\ k_{ji}^1 & k_{jj}^1 + k_{ii}^2 + k_{ii}^3 & k_{ij}^2 & k_{ij}^3 & 0 & 0 & 0 \\ 0 & k_{ji}^2 & k_{jj}^2 & 0 & 0 & 0 & 0 \\ 0 & k_{ji}^3 & 0 & k_{jj}^3 + k_{ii}^4 & 0 & k_{ij}^4 & 0 \\ 0 & 0 & 0 & 0 & k_{ii}^5 & k_{ij}^6 & 0 \\ 0 & 0 & 0 & k_{ji}^4 & k_{ji}^6 & k_{jj}^4 + k_{ii}^5 + k_{jj}^6 & k_{ji}^5 \\ 0 & 0 & 0 & 0 & 0 & k_{ji}^5 & k_{jj}^5 \end{pmatrix} \quad (1)$$

The first step for the load matrix was to obtain the matrices for the two plate elements subjected to distributed load. For this stage, the plate was considered as a double-clamped beam subjected to a decentralized distributed load. The values for elements 3 and 4 were used to calculate the equivalence of the load distributed at the nodes. Also, the equivalence of the localized load as a distributed load was calculated. For this purpose, the localized load value of 25 kN and the load application length (284 mm) were used. The final loading matrix was then assembled.

For the displacement matrix, the dimension was 21×1 , as each node has three degrees of freedom, one translational displacement, and two rotational displacements. Only nodes 1, 3, 5, and 7 will have zero displacement and rotation values. This was due to the boundary condition that delimits the clamping condition at these nodes.

The application of the MA method generated a linear system $F = K \delta$. The solve function from the SymPy[®] library was used to solve the developed equation system. Thus, displacement and reaction values were obtained. Additionally, the internal loads of elements 1, 2, and 3 were calculated. Due to the symmetry conditions of loading, geometry, and material, the internal load values of elements 1, 2, and 3 will be equal in elements 6, 5, and 4, respectively. The CAD drawing for the FEM simulation was created using SolidWorks[®] software, where the support base geometry was modeled in 3D. For the FEA, Ansys[®] software was used, more specifically the mechanical software, in which a static analysis was performed.

3. RESULTS AND DISCUSSION

Table 4 summarizes the values from the solution of the linear global system described.

Table 4. Displacements and reactions.

Variable	Value	Variable	Value
w_2	$-1,57309 \times 10^{-5} m$	R_{M1}	$-1317,41256 Nm$
φ_2	$0,0055170 rad$	R_{Z3}	$7553,92534 N$
θ_2	$-1,34781 \times 10^{-5} rad$	R_{T3}	$-51,88936 Nm$
w_4	$-0,00073091 m$	R_{M3}	$1746,33758 Nm$
φ_4	$-4,540150 \times 10^{-10} rad$	R_{Z5}	$4946,07714 N$
θ_4	$-1,34781 \times 10^{-5} rad$	R_{T5}	$39,14460 Nm$
w_6	$-1,57309 \times 10^{-5} m$	R_{M5}	$-1317,41307 Nm$
φ_6	$-0,0055170 rad$	R_{Z7}	$7553,92827 N$
θ_6	$-1,34781 \times 10^{-5} rad$	R_{T7}	$51,88934 Nm$
R_{Z1}	$4946,07523 N$	R_{M7}	$1746,33825 Nm$
R_{T1}	$-39,14460 Nm$	-	-

The bending moment applied was $1521.45 Nm$. This value is applied in Equation 2 to obtain the nominal bending stress at node 4.

$$\sigma_{nom} = \frac{(6 M)}{[(D - d)t^2]} = \frac{(6 \times 1521.45)}{[(0,30 - 0,12) \times 0.01905^2]} \quad (2)$$

$$\sigma_{nom} = 139.74 MPa.$$

The values of $d/D = 0.4$ and $d/t = 6.29$ imply $K = 1.3$ (UGURAL, 2018). Therefore, the maximum bending stress on the plate is calculated in Equation 3.

$$\sigma_{max} = \sigma_{nom} K = 139.74 \times 1.3 = 181.67 \text{ MPa} \quad (3)$$

Furthermore, the allowable stress is obtained by Equation 4:

$$\sigma_{adm} = S_y f_{dc} = 250 \times 0.9 = 230 \text{ MPa} \quad (4)$$

As the maximum stress in the plate is lower than the allowable one (a safety factor of 1.26 was obtained), it is concluded that the structure is adequate.

The stress in the beam is represented here by the web bending stress (Equation 5), which condition to calculate the referred stress is shown in Figure 4.

$$\sigma_{beam} = (M c) / I = [(12500 \times 0.051 \times (0.0062/2)] / [(1 \times 0.0062^3) / 12] \quad (5)$$

$$\sigma_{beam} = 99.50 \text{ MPa}$$

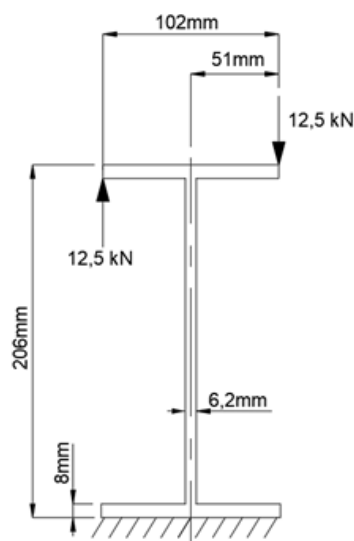


Figure 4. Web bending stress condition.

The solid body is generated in SolidWorks 2022[®]. In what refers to the FEA, only half of the geometry was represented due to symmetry condition. Furthermore, the resulting geometry was divided into two types of bodies: plate and beam. Subsequently, the geometry was exported to Ansys 2018[®], in which the previously discussed conditions were simulated.

In the simulation environment, the 12.5 kN-distributed load was applied in the upper region of the half-plate, to comply with the symmetry condition. As for the frames, the two

lower faces of the beam were used as fixed supports. Therefore, the symmetry condition was applied to the body. Also, the contact region between the two bodies was determined as bonded, that is, there is no relative displacement between the nodes connected between the two bodies.

The generated mesh presented 218339 nodes and 44244 elements. A maximum element size delimiter of 5 mm was applied and the mesh method chosen was hex-dominant (Figure 5).

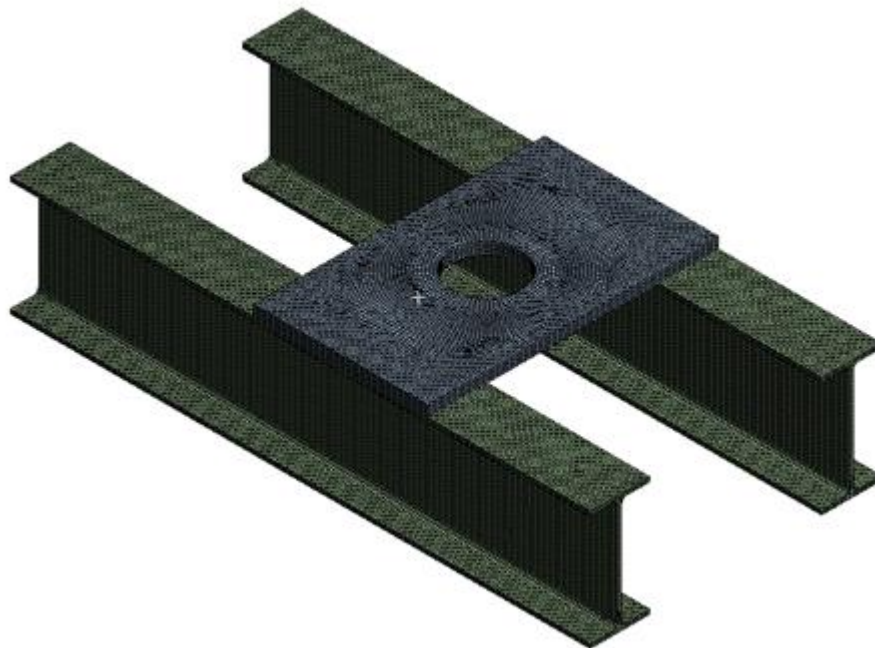


Figure 5. Simulation mesh.

Figure 6 and Figure 7 present the stress and displacement results obtained in the simulation for the beam and for the plate simultaneously. Table 5 summarizes the stresses and displacements at the previously calculated points in the plate and beam.

Table 5. Stresses and displacements from simulation in the plate and beam.

Component	Stress (MPa)	Displacement (mm)
Plate	172,44	0,92
Beam	95,46	0,35

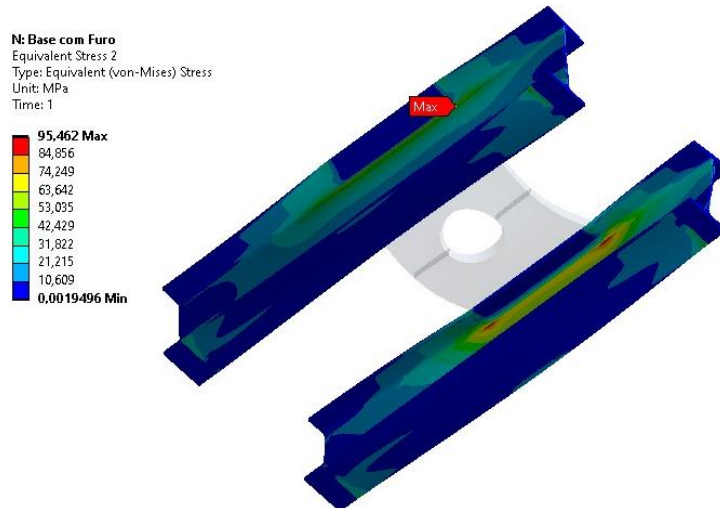


Figure 6. von Mises stress distribution with an indication of its maximum at the beam.

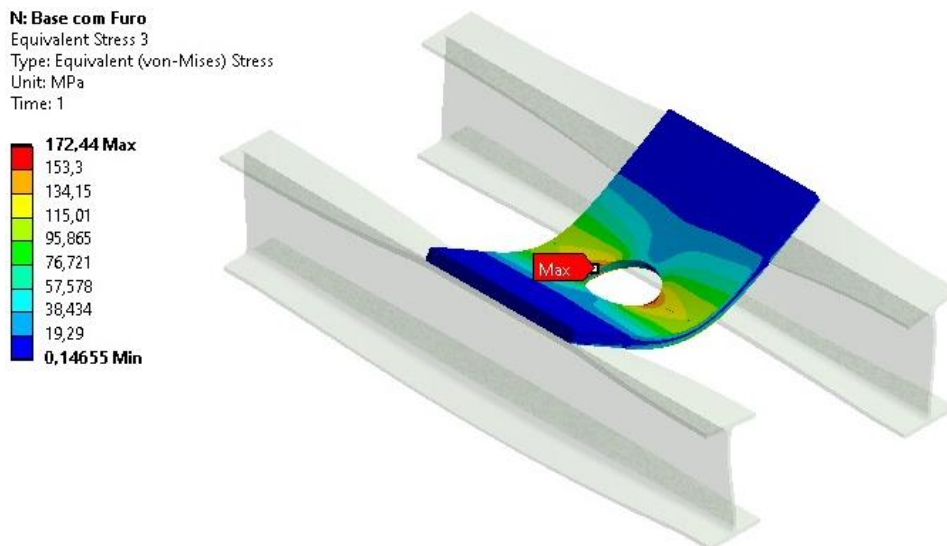


Figure 7. von Mises stress distribution with an indication of its maximum at the plate.

Table 6 establishes the comparison between the matrix and the FEM in what refers to stresses in the plate.

Table 6. Comparison between the matrix and the FEM.

Method	Stress at the plate (MPa)	Stress at the beam (MPa)
FEM	172,44	95,45
Matrix	181,76	99,50

It can be noted that there is a difference of 5.6% between the methods for bending stress values in the plate and 4.2% for the stress in the beam. The time to obtain these

results is described in Table 7. The analysis time related to MA represents only 11.59% of the time obtained via the finite element method with a loss of accuracy of 5.6% in stress.

Table 7. Comparison between the matrix and the FEM in what refers to the time to accomplish the calculation.

Method	Time (min)
FEM	30,2
Matrix	3,5

4. CONCLUSIONS

The research focused on the application of MA as a method for structural calculation, applied to the basic budgeting stage for the support base of the hydraulic gate drive piston. In addition, the aim was to reduce the time spent on this task. Regarding the activities addressed and developed in this paper, the following conclusions are reached:

1. The work was successful in reducing the time for structural calculation when comparing MA with the FEM, sacrificing a small difference in stress results between the compared methods.

2. The research adapted the MA method for structural verification of the base for hydraulic piston support to drive a hydraulic gate via the program written in Python®.

3. A comparison was made between the two methods analyzed and it was concluded that the stress difference for the analyzed case is small, and it is offset by the time saved for obtaining verification results. However, testing with more cases is necessary to be sure of the effectiveness of the application of the method.

Finally, it was concluded that the application of the MA method to replace the FEM for the budgeting stage is promising. However, to have confidence in the application of the method in practical situations, it is necessary to test more specific cases. This study is justified to ensure that the difference between stresses is not significant for all possible cases.

REFERENCES

AL-SHAWI, F. **Analysis of Structures by Matrix Methods**. Singapore: Jenny Stanford Publishing Pte, 2023. 532 p.

ANEEL - Agência Nacional de Energia Elétrica. **Brasil supera em 2022 os 8 GW de expansão na capacidade instalada**, 2023. Available in: <<https://www.gov.br/aneel/pt->

br/assuntos/noticias/2023/brasil-supera-em-2022-os-8-gw-de-expansao-na-capacidade-instalada#:~:text=em%20usinas%20solares.,Capacidade%20instalada,outorgados%20em%20fase%20de%20constru%C3%A7%C3%A3o>. Access in: April 4th, 2023.

ABNT - Associação Brasileira de Normas Técnicas. **ABNT NBR ISO 8883**: Cálculo e fabricação de comportas. Rio de Janeiro: ABNT, 2002, 68 p.

CALLISTER, W. D; RETHWISCH, D. G. **Ciência e Engenharia de Materiais: Uma introdução**. 8th ed. Rio de Janeiro: LTC, 2012. 844 p.

ERBISTI, Paulo C. F. **Design of Hydraulic Gates**. 2nd ed. Amsterdam: A. A. Balkema Publishers, 2008. 442 p.

GERDAU. **Perfis Gerdau**, 2023. Available in: <<https://mais.gerdau.com.br/catalogos-e-manuais?type=catalogos-e-manuais&cat=segmentos&s=perfis>>. Access in: April 6th, 2023.

LI, Y.; LUO, Z. A Reduced-Dimension Extrapolating Method of Finite Element Solution Coefficient Vectors for Fractional Tricomi-Type Equation. **Mathematics**, v. 11 (4699), p. 1-13, 2023.

LUO, Z.; JIANG, W. A reduced-order extrapolated technique about the unknown coefficient vectors of solutions in the finite element method for hyperbolic type equation. **Applied Numerical Mathematics**, v. 158, p. 123-133, 2020.

TENG, F.; LUO, Z. A reduced-order extrapolated approach to solution coefficient vectors in the Crank-Nicolson finite element method for the uniform transmission line equation. **Journal of Mathematical Analysis and Applications**, v. 493 (124511), p. 1-13, 2021.

TIMOSHENKO, S. **Mecânica dos sólidos: Volume I**. 1st ed. Rio de Janeiro: LTC, 1984. 258 p.

UGURAL, A. **Plates and Shells**. 4th ed. London: Taylor & Francis Group, 2018. 618 p.

ZENG, Y.; LUO, Z. The reduced-dimension technique for the unknown solution coefficient vectors in the Crank–Nicolson finite element method for the Sobolev equation. **Journal of Mathematical Analysis and Applications**, v. 513 (126207), p. 1-13, 2022.